

EXAFS and IR Structural Study of Platinum-Based Anticancer Drugs' Degradation by Diethyl Dithiocarbamate

Diane Bouvet,^{*,†} Alain Michalowicz,[†] Sylvie Crauste-Manciet,^{‡,§} Denis Brossard,^{‡,§} and Karine Provost[†]

Laboratoire de Physique Structurale des Molécules et Matériaux, Université Paris XII, 61 avenue du Général De Gaulle, 94010 Créteil Cedex, France, Laboratoire de Pharmacie Galénique, Université Paris V, 75006 Paris, France, and Service de Pharmacie, CHI Poissy Saint Germain en Laye, 78105 Saint Germain en Laye, France

Received November 3, 2005

Platinum compounds constitute a discrete class of DNA-damaging anticancer drug agents, including cisplatin, carboplatin, and oxaliplatin. The toxicity of such drugs raises the problem of waste detoxification. Diethyl dithiocarbamate (DDTC) is recommended by the World Health Organization (WHO) for the destruction of cisplatin, but the degradation product has not been structurally characterized. This paper deals with the extended X-ray absorption fine structure (EXAFS) and IR structural study of the reaction products of DDTC with cisplatin, carboplatin, and oxaliplatin. Cisplatin and carboplatin give the same reaction product: Pt(DDTC)₂. In the case of oxaliplatin, we observed the formation of [(diaminocyclohexane)(DDTC)Pt(II)]. In all cases, the replacement of labile ligands by strong ligands should lead to inactive compounds. Our results suggest that the WHO inactivation protocol might be extended to carboplatin and oxaliplatin. Nevertheless, this should be validated by toxicity tests of the degradation products.

Introduction

Platinum compounds constitute a discrete class of DNA-damaging anticancer agents, and their clinical uses are now widespread. The first platinum coordination complex introduced in 1972 as a cytotoxic agent was cisplatin.^{1,2} Clinical experience has shown that cisplatin is highly nephrotoxic and presents intrinsic and/or acquired tumor resistance, leading to the development of other platinum compounds.

Carboplatin [diamine(1,1-cyclobutanedicarboxylato(2-)-O,O')-platinum(II)] is a second generation platinum antitumor drug used in the same type of cancers as cisplatin.³ In this platinum(II) complex, the metallic ion is bonded in the cis position to two amines and chelated by a cyclobutanedicarboxylate ligand, as shown in Figure 1 b.

Oxaliplatin *cis*-[(1*R*,2*R*)-1,2-cyclohexanediamine-*N,N'*]-[oxalato(2-)-O,O']platinum(II) is a third-generation platinum

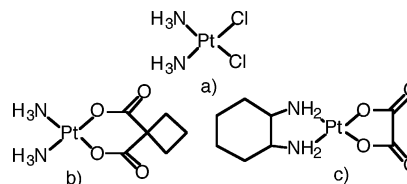


Figure 1. Formulas of (a) cisplatin, (b) carboplatin, and (c) oxaliplatin.

antitumoral drug approved for metastatic carcinoma treatments.⁴ Oxaliplatin is formed by a platinum(II) ion chelated by two bidentate ligands: one diaminocyclohexane (DACH) and one oxalate (ox), as shown in Figure 1c.

Carboplatin has been shown to be less toxic than cisplatin and equally active.^{3,5} However, it presents a cross-resistance with the first generation drug. In preclinical studies, oxaliplatin has demonstrated efficacy on a broad spectrum of experimental tumors, including cisplatin- and carboplatin-resistant cell lines.^{4,6}

Sodium diethyl dithiocarbamate (DDTC) [(C₂H₅)₂NCS₂⁻-Na⁺] is recommended by the World Health Organization for

* To whom correspondence should be addressed. E-mail: bouvet@univ-paris12.fr.

[†] Laboratoire de Physique Structurale des Molécules et Matériaux, Université Paris XII.

[‡] Laboratoire de Pharmacie Galénique, Université Paris V.

[§] Service de Pharmacie, CHI Poissy Saint Germain en Laye.

(1) Rosenberg, B.; Camp, L. V.; Krigas, T. *Nature* **1965**, *205*, 698.

(2) Jamieson, E. R.; Lippard, S. J. *Chem. Rev.* **1999**, *99*, 2467.

(3) Micetich, K. C.; Barnes, D.; Erickson, L. C. *Cancer Res.* **1985**, *45*, 4043.

(4) Graham, M. A.; Lockwood, G. F.; Greenslade, D.; Brienza, S.; Bayssas, M.; Gamelin, E. *Clin. Cancer Res.* **2000**, *6*, 1205.

(5) Kelland, L. R.; Sharp, S. Y.; O'Neill, C.; Raynaud, F. I.; Beale, P. J.; Judson, I. R. *J. Inorg. Biochem.* **1999**, *77*, 111.

(6) Desoize, B.; Madoulet, C. *Crit. Rev. Oncol./Hematol.* **2002**, *42*, 317.

the destruction of cisplatin in different wastes, such as glassware, aqueous solutions, or spills,⁷ on the basis of the absence of mutagenic activity of the residue. Furthermore, pharmacological studies have shown that the salt NaDDTC is effective in reducing several kinds of nephrotoxicity when administered just after a cisplatin injection.^{8,9} Nevertheless the structures of the degradation products are still unknown. Moreover, to our knowledge, there is no similar recommendation for other platinum compounds such as carboplatin and oxaliplatin. We have thus undertaken the structural study of these three drugs' reaction products with DDTC.

Up to now, we have not obtained any crystal suitable for an X-ray diffraction study. Thus, we applied X-ray absorption spectroscopy (XAS), which has already proved to be a reliable technique, for studying the platinum local structure in similar structural problems.^{10–12} The extended X-ray absorption fine structures (EXAFSs) of the three native drugs and their degradation products with chloride ions have already been studied,¹² and their XAS features are fully understood. Following this previous work, this paper deals with the structural studies of the three drugs' degradation by DDTC.

Experimental Section

Samples Preparation. Cisplatin, carboplatin, and oxaliplatin were obtained from pharmaceutical preparations, respectively, from Qualimed, Merck, and Sanofi. Carboplatin and oxaliplatin were diluted to 10 mg/mL and cisplatin was diluted in microfiltrated water to 1 mg/mL, with respect to their solubilities. Each compound is mixed in solution with a large excess of diethyl dithiocarbamate (0.33 M). Thus, the reaction is expected to be complete.

For 1 mL of each solution, a yellow precipitate immediately appears under these conditions. The precipitates were washed three times in water, separated by centrifugation at 8000 rpm, and dried in an oven at 60 °C for 2 days before XAS measurement. The XAFS spectra of the supernatant liquid do not show any Pt(II)LIII edge jump within the error bars. This proves that >99% of platinum has precipitated.

Infrared Measurements. About 1–2 mg of each degradation product of cisplatin, carboplatin, and oxaliplatin was prepared as KBr pellets. The mixed products were compressed under vacuum in order to make the pellets transparent to infrared radiation up to 400 cm⁻¹. Each pellet spectrum (including the KBr reference pellet) was recorded with an IRTF Perkin-Elmer spectrometer BX II, in the range 6000–450 cm⁻¹, with a 2 cm⁻¹ resolution.

XAS Measurements and Analysis. Precipitates were prepared as compressed pellets of a homogeneous mixture

of pure product and cellulose. The quantities of products were calculated in order to obtain an edge jump $\Delta\mu x$ near 1, with a total absorbance after the edge $\mu x(E) < 2$.

Precipitate spectra were recorded in transmission mode at LURE (the French synchrotron radiation facility), with the following experimental conditions: LIII Pt edge and energy range 11 450–12 600 eV. Precipitates with carboplatin and oxaliplatin spectra were recorded on the EXAFS13 station, with a Si(111) channel-cut monochromator. Precipitate with cisplatin spectrum was recorded on the EXAFS2 station, with a Si(111) double crystal monochromator. The EXAFS spectra were extracted using the standard procedures^{13–15} available in the program "Exafs pour le Mac",¹⁶ including spline-smoothing atomic absorption determination, energy-dependent normalization, and fast Fourier transform (FT) ($E_0 = 11 560$ eV, FT range = 2–14 Å⁻¹). Each spectrum was recorded three times and averaged.

Since the three native drugs have already been characterized, they were used as model compounds. Structural models for unknown compounds are based on the methodology established for the known model compounds.¹²

EXAFS modeling of the complete structures was performed in three steps:

(i) Fourier filtering of the main peak and fitting of the EXAFS contribution of the neighbors directly bonded to platinum. The aim of this preliminary fit is to determine the type and number of first Pt(II) neighbors.

(ii) Construction of the molecular models with the Chem3D program using characteristic crystallographic distances and the knowledge of the ligand structures. Preparation of the resulting FEFF¹⁷ input files with the code CRYSTALFF.¹⁸

(iii) Ab initio EXAFS modeling with FEFF7. Sorting of the most important single and multiple scattering paths. Equivalent paths are grouped in order to fit with a single amplitude-phase function. Several models of ligand binding are tested and, when parameters are physically acceptable, quantitatively compared using the statistical *F*-test.^{19,20}

All the fits of steps (i) and (iii) are performed with Round Midnight code¹⁶ by comparing the experimental spectra to the EXAFS standard formula (eq 1).

$$k\chi(k) = -S_0^2 \sum_i \frac{N_i}{R_i^2} |f_i(k, R_i)| e^{-2\sigma_i^2 k^2} e^{-2R_i/\lambda(k)} \sin[2kR_i + 2\delta_1(k) + \psi_i(k)] \quad (1)$$

The sum is done on the most important selected single and multiple scattering paths. S_0^2 is the amplitude reduction

(7) Castegnarò, M. *OMS–IARC Sci. Publ.* **1985**, 73, 97.

(8) Reedjik, J. *Chem. Rev.* **1999**, 99, 2499.

(9) Bodenner, D. L.; Dedon, P. C.; Keng, P. C.; Borch, R. F. *Cancer Res.* **1986**, 46, 2745.

(10) Curis, E.; Provost, K.; Nicolis, I.; Bouvet, D.; Benazeth, S.; Crauste-Manciet, S.; Brion, F.; Brossard, D. *New J. Chem.* **2000**, 24, 1003.

(11) Curis, E.; Provost, K.; Bouvet, D.; Nicolis, I.; Crauste-Manciet, S.; Brossard, D.; Benazeth, S. *J. Synchrotron Radiat.* **2001**, 8, 716.

(12) Bouvet, D.; Provost, K.; Crauste-Manciet, S.; Curis, E.; Nicolis, I.; Brossard, D.; Michalowicz, A. *J. Synchrotron Radiat.* **2005**, in press.

(13) Teo, B. K. *Inorganic Chemistry concepts, EXAFS: Basic Principles and Data analysis*; Berlin, 1986.

(14) Koenigsberger, D. C.; Prins, R., Eds. John Wiley: New York, 1988.

(15) Lytle, F. W.; Sayers, D. E.; Stern, E. A. *Physica B* **1989**, 158, 701.

(16) Michalowicz, A. *J. Phys. IV* **1997**, 7, 235.

(17) Rehr, J. J.; Zabinski, S. I.; Alberts, A. C. *Phys. Rev. Lett.* **1992**, 69, 3397.

(18) Provost, K.; Champloy, F.; Michalowicz, A. *J. Synchrotron Radiat.* **2001**, 8, 1109.

(19) Joyner, R. W.; Martin, K. J.; Meehan, P. J. *J. Phys.* **1987**, C20, 4005.

(20) Michalowicz, A.; Provost, K.; Laruelle, S.; Mimouni, A.; Vlais, G. *J. Synchrotron Radiat.* **1999**, 6, 233.

factor, and N_i is the number of equivalent scattering paths with an effective distance R_i . $\lambda(k)$ is the mean-free path of the photoelectron. σ_i is the Debye–Waller coefficient, characteristic of the distance distribution width for path i . $\delta_1(k)$ is the central atom phase shift, and $|f_i(k)|$ and $\psi_i(k)$ are the amplitude and phase for the neighbor scattering factors, calculated by FEFF7 code. Since theoretical phase shifts and amplitudes were used, it is necessary to fit the energy threshold E_0 . The photoelectron mean-free path is set to the empirical formula (eq 2),

$$\lambda(k) = \frac{1}{\Gamma} \left[k + \left(\frac{\eta}{k} \right)^4 \right] \quad (2)$$

Values for Γ and η are set to $\eta = 3.1$ and $\Gamma = 0.7$, as established in our previous study.¹² In the modeling of the filtered first coordination sphere, we have fitted separated Debye–Waller (DW) factors σ_i for each type of atom. For the fit of the complete spectra, it was necessary to limit the total number of fitted parameters in order to limit the correlations and improve the fitting statistics. Thus, it was decided to fit a global DW factor for all the shells. In all cases, a global ΔE_0 was refined.

The goodness of fit, or quality factor, is $QF = \Delta\chi_{\min}^2/\nu$, where $\Delta\chi_{\min}^2$ is the minimum value of the statistical $\Delta\chi_{\text{stat}}^2$ (eq 3) and the degree of freedom $\nu = N_{\text{ind}} - N_{\text{par}}$, where N_{ind} is the number of independent points and N_{par} is the total number of fitted parameters.

$$\Delta\chi_{\text{stat}}^2 = \frac{N_{\text{ind}}}{N_{\text{pt}}} \sum_i \frac{[k\chi_{\text{th}}(i) - k\chi_{\text{exp}}(i)]^2}{\epsilon_i^2} \quad (3)$$

In eq 3, N_{pt} is the number of experimental points and ϵ_i^2 is the experimental error. Statistical errors on the average spectra and error bars of the fitted parameters are evaluated as recommended by the IXS Standard and Criteria subcommittee.²¹

The EXAFS spectra are fitted in the range 3–14 \AA^{-1} . The R -space fitted range is 1–3 \AA for the first shell fits and 1–5 \AA for the complete spectra. The numbers of independent points $N_{\text{ind}} = 2\Delta k\Delta R/\pi$ are, respectively, 14 and 28. The average experimental error is evaluated to be $\langle \epsilon \rangle = 0.015$.

Results and Discussion

Experimental Spectra. The EXAFS experimental signals of the three precipitates are presented in Figure 2. Signals (a), (b), and (c) correspond to the products of reaction between and cisplatin, carboplatin, and oxaliplatin, respectively. As a control, signals of the three drugs before reaction are represented in dotted lines. The corresponding Fourier transforms (without phase-shift correction) are presented in Figure 3. The evolution of the EXAFS spectra and their Fourier transforms for the three drugs upon degradation by DDTC reflects the huge changes induced in the Pt(II) coordination sphere by this sulfur ligand.

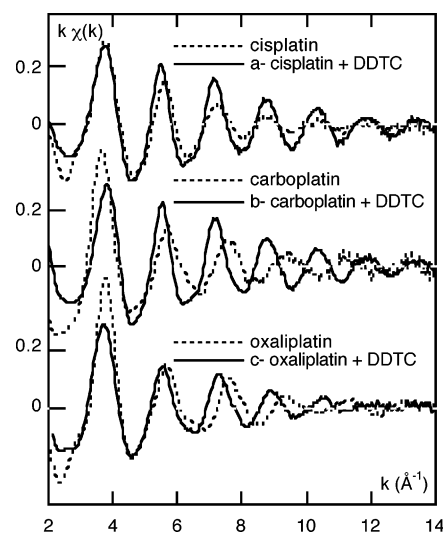


Figure 2. Comparison of EXAFS spectra before and after reaction between DDTC and cisplatin, carboplatin, or oxaliplatin.

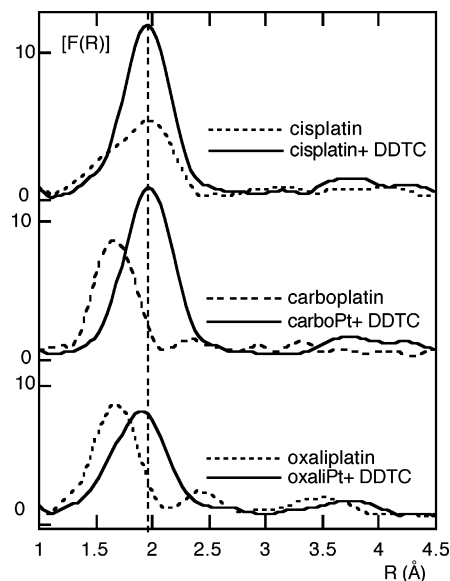


Figure 3. Comparison of Fourier transform amplitudes before and after reaction between DDTC and cisplatin, carboplatin, or oxaliplatin.

For cisplatin, the apparent modification is represented by an important raise of the FT amplitude without any significant change of the average Pt–ligand distance. On the contrary, both carboplatin and oxaliplatin first shell radial distribution functions are shifted to a greater distance. In carboplatin, this distance shift is accompanied by an important increase of the amplitude, while this amplitude is apparently not significantly affected for oxaliplatin.

The FT spectra of the three modified compounds show a common new feature, when compared to the native one: a relatively intense peak appears around 4 \AA . In the case of oxaliplatin, this outbreak comes with the fading of a peak at 3.5 \AA , which has been previously shown to be the signature of the oxalate ligand.¹²

At least, the EXAFS spectra and Fourier transforms of DDTC-degraded cisplatin and carboplatin are superimposable within the error bars: both compounds should be modeled with the same short-range order. On the contrary, the

(21) IXS. Report on errors in EXAFS fitting. http://ixs.iit.edu/subcommittee_reports/sc/ (accessed March 16, 2006).

spectrum and the local structure of the oxaliplatin degradation product are significantly different.

These qualitative observations can be rationalized in order to guide the first guess of the quantitative models and refinements developed in the modeling section. The native coordination sphere of Pt(II) in cisplatin is composed of two nitrogen and two chlorine atoms, while both native carboplatin and oxaliplatin have a *cis*-PtN₂O₂ coordination sphere. Adjacent atoms in the periodic table, such as sulfur and chlorine on one hand and nitrogen and oxygen on the other hand, are known to have very close EXAFS signals. Moreover, the Pt–Cl and Pt–S bond length found in the literature are in the same range (2.2–2.4 Å), while the common range for both Pt–N and Pt–O bond lengths is 1.95–2.05 Å. The replacement of a chlorine atom by a sulfur atom should not change significantly the corresponding EXAFS signal, while the replacement of a light atom (N/O) should induce a huge change.

In the case of DDTC-degraded cisplatin, the doubling of the main peak amplitude suggests that the two nitrogens, at least, must have been substituted by sulfur atoms, leading to a PtS₄ or a PtS₂Cl₂ coordination sphere. Because Cl[–] ligands are more labile than amines, the first solution is much more likely. Furthermore, the carboplatin degradation product has been obtained in the absence of any chloride ions. Thus, the platinum environment can only be composed of nitrogen, oxygen, and sulfur atoms. Because DDTC-degraded cisplatin and carboplatin Fourier transforms are superimposable up to 5 Å, we expect that, in both products, the Pt(II) ion has a PtS₄ first coordination sphere.

In the case of the oxaliplatin degradation product, no huge increase of the main peak in the Fourier transform was observed. Because both ligands in oxaliplatin are bidentate, we expect that only one ligand may have been displaced, leading to a Pt(N/O)₂S₂ coordination sphere. The absence of the oxalate signature in the DDTC-degraded oxaliplatin spectrum suggests that the oxalate is displaced while the DACH remains bonded to the Pt(II) center.

EXAFS Modeling of the First Coordination Sphere. As quoted before, the coordination spheres of cisplatin (or carboplatin) and oxaliplatin are drastically modified upon reaction with DDTC. In both cases, the type and the number of atoms in the first shell were determined using the method recommended by Penner-Hahn and co-workers²² and modified by Michalowicz et al.²⁰ A PtN_{4–x}S_x model has been tested, where *x* is a whole number varying from 0 to 4. For each value of *x*, the Debye–Waller factor σ and bond lengths *R* were fitted. The goodness of fit was estimated using the quality factor QF. Table 1 presents the variation of quality factor versus *x* in the fitting of the first coordination sphere of cisplatin/carboplatin and oxaliplatin degradation products with a PtN_{4–x}S_x model. The models and the parameters of the best simulations are reported in Table 2.

In the case of cisplatin or carboplatin degradation products, the first sphere signal is fitted with a four-sulfur-atom model.

Table 1. Evolution of the Quality Factor (QF) Versus the Composition of the PtN_{4–x}S_x Coordination Sphere (Best Corresponds to the Lowest QF)

PtN _{4–x} S _x <i>x</i>	cisplatin/carboplatin QF	oxaliplatin QF
0	30.5	7.52
1	14.0	1.48
2	3.80	1.41
3	3.27	2.05
4	1.94	2.79

Table 2. Fit Parameters of the First Coordination Shell for the Precipitates

path	<i>N</i>	$\sigma \times 10^2$ (Å)	<i>R</i> (Å)	\bar{R} (Å)
Cisplatin/Carboplatin and DDTC				
Pt–S	4	5.6 (2)	2.31 (1)	<i>R</i> _{XR} = 2.32
residual = 3.23×10^{-2} , <i>N</i> _{par} = 2, QF = 1.94, ΔE = 7.5 eV				
Oxaliplatin and DDTC				
Pt–N/O	2	5.5 (4)	2.05 (1)	<i>R</i> _{XR} = 2.04
Pt–S	2	5.4 (3)	2.29 (1)	<i>R</i> _{XR} = 2.32
residual = 5.36×10^{-2} , <i>N</i> _{par} = 4, QF = 1.41, ΔE = 7.5 eV				

For oxaliplatin DDTC precipitate, the best fit is obtained with two light atoms (O or N) and two sulfur atoms. These quantitative results confirm the qualitative assumptions presented in the previous section. As expected, the platinum environment after reaction presents a huge difference between cisplatin/carboplatin and oxaliplatin. All fitted distances are coherent with PtN or PtS crystallographic distances found in the literature for similar complexes.^{23–25}

Structural Characterization of the Pt–DDTC Bonding Mode by IR Spectroscopy. The reaction of the DDTC ligand with cisplatin and carboplatin leads to the formation of four Pt–S bonds, while two Pt–S bonds are involved in the degradation product of oxaliplatin. Structures of different dithiocarbamate (DTC) metal complexes have proved that DTC can bind the metal ion either in a monodentate mode or in a bidentate one.^{24–28} Nevertheless, the EXAFS refinement of the first coordination sphere is unable to distinguish both modes of fixation.

To discriminate between monodentate and bidentate DDTC binding on Pt, we have decided to examine the IR spectra of the degradation product. We have restricted our IR analysis to the C–S vibrational IR signal of these compounds. Nakamoto²⁹ and Manav et al.²⁸ have shown that the C–S vibration band around 1000 cm^{–1} in the IR spectra of DTC metal complexes is a good way to distinguish both binding modes. When the Pt–DTC binding is monodentate, the two C–S vibration modes are different and the elongation mode should occur as a doublet separated by 20 cm^{–1}.²⁸ On the contrary, the bidentate Pt–DTC binding mode is sym-

(23) Hansson, C.; Kukushkin, V. Y.; Lövgqvist, K.; Yong, S.; Oskarsson, A. *Acta Crystallogr.* **2003**, C59, m432.

(24) Heath, G. A.; Hockless, D. C. R.; Prenzler, P. D. *Acta Crystallogr.* **1996**, C52, 537.

(25) Christidis, P. C.; Rentzeperis, P. J. *Acta Crystallogr.* **1979**, B35, 2543.

(26) Faraglia, G.; Fedrigo, M. A.; Sitran, S. *Transition Met. Chem.* **2002**, 27, 200.

(27) Marzano, C.; Bettio, F.; Baccichetti, F.; Trevisan, A.; Giovagnini, L.; Dregona, D. *Chem.-Biol. Interact.* **2004**, 148, 37.

(28) Manav, N.; Mishra, A. K.; Kaushik, N. K. *Spectrochim. Acta, Part A* **2004**, 60, 3087.

(29) Nakamoto, K. *Infrared and Raman spectra of inorganic and coordination compounds, 3th ed.*; John Wiley & Sons: New York, 1978.

(22) Clark-Baldwin, K.; Tierney, D. L.; Govindaswamy, N.; Gruff, E. S.; Kim, C.; Koch, S. A.; Penner-Hahn, J. E. *J. Am. Chem. Soc.* **1998**, 120, 8401.

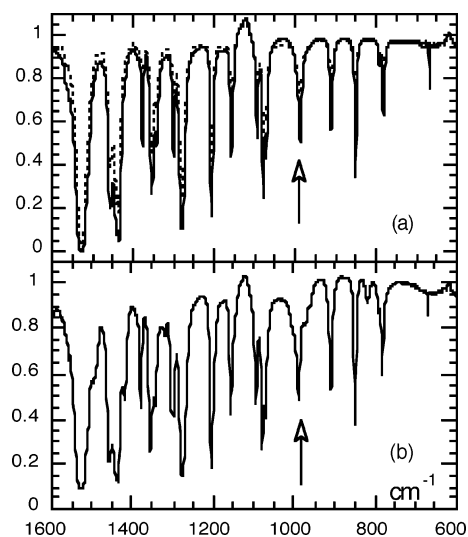


Figure 4. Infrared spectrum of (a) cisplatin (dotted lines)/carboplatin–DDTC degradation products and (b) oxaliplatin–DDTC degradation product.

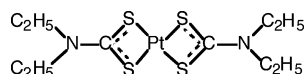


Figure 5. Model for precipitates obtained with carboplatin and cisplatin.

Table 3. Fit Parameters of the Degradation Product of Carboplatin or Cisplatin in the Presence of DDTC

path	<i>N</i>	$\sigma \times 10^2$ (Å)	<i>R</i> (Å)
Pt–S	4	4.9 (1)	2.31 (1)
Pt–C	2	4.9 (1)	2.84 (2)
Pt–C–N'	2	4.9 (1)	4.12 (1)
Pt–S–Pt–S	4	4.9 (1)	4.59 (1)
residual = 1.84×10^{-2} , $N_{\text{par}} = 6$, QF = 2.17, $\Delta E = 7.7$ (1) eV			

metric and should be detected as a single C–S vibration band.

Parts a and b of Figure 4 display, respectively, the superimposed IR spectra of DDTC-degraded cisplatin and carboplatin and the oxaliplatin degradation product IR spectrum. As expected, the cisplatin and carboplatin IR spectra are very similar, while some differences appear for oxaliplatin. In both figures, the elongation C–S characteristic vibration mode is a singlet. Thus, we can assume that the Pt–DDTC ligand binding mode is bidentate for the three compounds.

EXAFS Model for DDTC-Degraded Carboplatin/Cisplatin. Figure 5 presents the only acceptable model with a 4S coordination sphere and a bidentate fixation of the ligand. The complete EXAFS spectrum of this reaction product can be modeled *ab initio* up to 5 Å using FEFF7 code. An analysis of the most important scattering-path contributions showed that it was possible to limit the refinement of the platinum neighborhood to four groups of paths, as shown in Table 3. The two first groups correspond to single scattering paths Pt–S and Pt–C. The third group takes into account the multiple scattering path through the alignment PtCN'. In the later one, we used multiple scattering paths through the platinum ion. These scattering paths are represented in Figure 6. After XAFS refinement, the final model is coherent with the already-fitted Pt–S distance and with the known

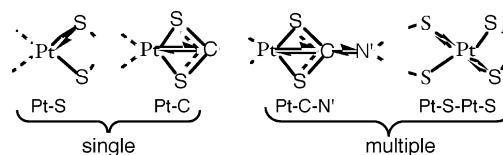


Figure 6. Most important scattering paths of the carboplatin degraded EXAFS signal.

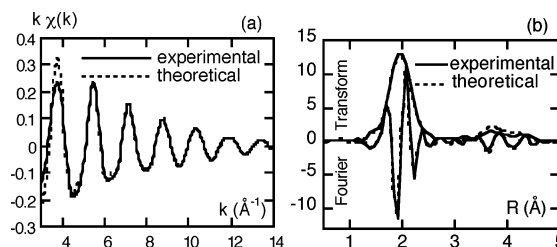


Figure 7. Comparison between experimental and theoretical signals for carboplatin degraded by DDTC: (a) EXAFS spectrum and (b) corresponding FT.

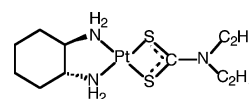


Figure 8. Model for precipitate obtained for oxaliplatin.

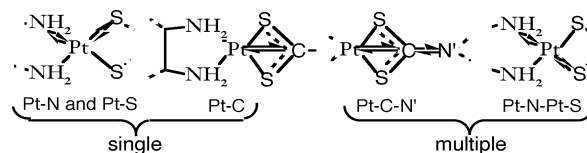


Figure 9. Most important scattering path for the oxaliplatin degraded EXAFS signal

geometry of the DDTC bidentate ligand.^{24,25} All other parameters present physical acceptable values.

The comparison between experimental and refined FEFF-simulated EXAFS spectra of cisplatin and DDTC degradation product, and their respective FT, is presented in Figure 7. The four-shell model detailed above fits to the complete EXAFS spectrum within the error bars. Moreover, the FT contribution around 4 Å is well-reproduced if we take into account both multiple scattering groups: Pt–C–N' and Pt–S–Pt–S. The 4 Å multiple scattering signals of carboplatin and cisplatin degraded by DDTC are identical. This result definitely rules out the possibility of a PtS₂Cl₂ structure: in such a hypothetical model, the 4 Å signal should be less intense.

EXAFS Model for DDTC-Degraded Oxaliplatin. As discussed above, the signature of oxalate ligand binding at 3.5 Å is missing after reaction. This suggests that this ligand is displaced by DDTC. We have already shown in the IR section that the Pt–DDTC bond is bidentate. According to these results, we propose that, in the degradation complex, the platinum ion is bonded to both bidentate DACH and DDTC ligands, as shown in Figure 8.

The oxaliplatin degradation product EXAFS spectrum can be reproduced with a five-shell FEFF model. Figure 9 presents the scattering-paths scheme. The first three shells correspond to single scattering paths Pt–N, Pt–S, and Pt–C (one for DDTC and two for DACH). The two later ones take into account multiple scattering paths, respectively,

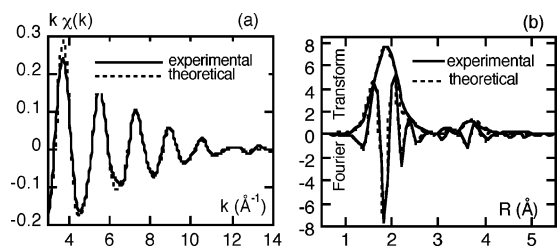


Figure 10. Comparison between experimental and theoretical signals for oxaliplatin degraded by DDTC: (a) EXAFS spectrum and (b) corresponding FT.

Table 4. Fit Parameters of the Degradation Product of Oxaliplatin in the Presence of DDTC

path	N	$\sigma \times 10^2$ (Å)	R (Å)
Pt–N	2	4.77 (4)	2.04 (1)
Pt–S	2	4.77 (4)	2.28 (1)
Pt–C	3	4.77 (4)	2.80 (2)
Pt–C–N'	2	4.77 (4)	4.13 (3)
Pt–N–Pt–S	2	4.77 (4)	4.26 (3)

residual = 2.96×10^{-2} , $N_{\text{par}} = 7$, $QF = 1.45$, $\Delta E = 6.4$ (3) eV

through the PtCN' alignment and through the central atom. Compared to these multiple scattering paths, the EXAFS signals corresponding to the DACH ligand outer shells can be neglected.

It appears that the common feature observed around 4 Å in the three modified drug spectra is essentially due to the Pt–C–N' multiple scattering focusing effect. The best simulation parameters are presented in Table 4. As for cisplatin/carboplatin, the complete model distances are in good agreement with the already fitted Pt–S and Pt–N distances and with the known geometry of the DDTC bidentate ligand. With such parameters, the EXAFS spectrum and its Fourier transforms are well-reproduced (Figure 10).

Conclusion

The detoxification of cisplatin by the DDTC process is already validated. Our EXAFS and IR study completes the knowledge of this process by the structural characterization of the final nontoxic compound, despite the difficulty to obtain monocrystals. The Pt(II) coordination sphere has been completely substituted by two bidentate sulfur bonds, leading

to a centro-symmetric square planar PtS₄ structure. The replacement of the two Pt–amine and the two labile Pt–chlorine bonds in a cis geometry by four Pt–S bonds may explain the absence of anticancer activity and toxicity. The resulting complex might not be hydrolyzed and fixed specifically on the DNA chain.

The local EXAFS structure of the carboplatin–DDTC degradation product is the same as that for cisplatin–DDTC. Furthermore, their IR spectra are identical. Thus, we can assume that both drugs lead to the same final product. This result suggests that the detoxification process already recommended for cisplatin might be extended to carboplatin.

The structural feature of oxaliplatin–DDTC is quite different: DDTC substitutes only the oxalate ligand. We have shown elsewhere that the oxalate ligand is labile in Pt(II) complexes.¹² The present work confirms that it is more labile than DACH.³⁰ The binding of oxaliplatin to DNA is assumed to be preceded by the hydrolysis of oxalate. Its substitution by a strong ligand like DDTC should also lead to a nontoxic and nonactive compound.

In summary, our results suggest that DDTC might be a good candidate for the inactivation of carboplatin and oxaliplatin. Nevertheless, this should be validated by activity and toxicity tests.

Various nucleophilic sulfur ligands are proposed in different biological and clinical processes involving platinum-based anticancer drugs. The EXAFS structural study of these reactions, either precipitates or still in solution, is under investigation and will be published later.

Acknowledgment. We would like to thank Pr. Simone Benazeth, Dr. Jacques Moscovici, Dr. Emmanuel Curis, and Dr. Ioannis Nicolis for data collection at LURE, and Dr. Nicolas Fray and Dr. Hervé Cottin for IR data collection, as well as all their helpful discussions. The financial support by the French Ministry of Education is gratefully acknowledged.

IC051904U

(30) Wong, E.; Giandomenico, C. M. *Chem. Rev.* **1999**, *99*, 2451.